Dynamic Aspects of the Contractile System in *Physarum* Plasmodium. III. Cyclic Contraction–Relaxation of the Plasmodial Fragment in Accordance with the Generation–Degeneration of Cytoplasmic Actomyosin Fibrils

Mitsuo Ishigami,* Kiyoko Kuroda,‡ and Sadashi Hatano§

*Department of Biology, Faculty of Education, Shiga University, Otsu, Shiga 520, Japan; ‡Department of Biology, Faculty of Science, Osaka University, Toyonaka, Osaka 560, Japan; §Institute of Molecular Biology, Faculty of Science, Nagoya University, Chikusa-ku, Nagoya 464, Japan

Abstract. Plasmodial fragments of *Physarum polycephalum*, excised from anterior regions of a thin-spread plasmodium, contracted–relaxed cyclicly with a period of 3–5 min. The area of the fragments decreased ~10% during contraction. In most cases, there was little endoplasmic streaming which indicates that contractions were synchronized throughout the fragment. By both polarized light and fluorescence microscopy, the organization and distribution of the cytoplasmic actomyosin fibrils in the fragments changed in synchrony with the contraction cycle. The fibrils formed during the contraction phase, and finally became a highly organized framework consisting of a three-dimensional network of numerous fibrils with many converging points (the nodes). During relaxation, the fibrils degenerated and disappeared almost completely, though some very weak fibrils remained near the nodes and the periphery. The results obtained by fluometry of the fragments, stained with rhodamine-phalloidin, suggested that the G-F transformation of actin is not the main underlying process of the fibrillar formation.

THE cytoplasmic actomyosin fibrils in the *Physarum* plasmodium intimately participate in the generation of motive force (1–4, 8, 10–12, 15, 17, 18, 23, 28). However, the morphodynamics of the fibrils have not been sufficiently elucidated in connection with the contractility of the plasmodium.

Wohlfarth-Bottermann and his co-workers (6, 30, 31) observed by electron microscopy that the fibrils were newly generated in the hanging plasmodial strand at the contraction phase and degraded at the relaxation phase. On the other hand, Nagai et al. (24) asserted that well-developed microfilament bundles (cytoplasmic fibrils) formed at the early phase of contraction as the result of changes in the aggregation pattern of F-actin, and that they transformed into kinky aggregates at the maximum contraction. The disagreement between these observations about the morphodynamics of the fibrils has not been resolved.

Cytoplasmic fibrils in the anterior region of a thin-spread plasmodium appear–disappear cyclicly coupled with the shuttle streaming (9, 11, 13, 25). However, it is hard to determine definitely the phase of the contraction cycle from the streaming direction (9), because the endoplasmic flow is caused by the difference in the local inner pressure (15). To elucidate the morphodynamics of the fibrils related to the contractility, a system must be developed to represent simultaneous indications both for the morphological change of the fibrils and the phase change of the contraction cycle. Using plasmodial fragment, we were able to clarify the phase relationship of the two cycles.

Materials and Methods

Preparation of Plasmodial Fragment

Plasmodia of *Physarum polycephalum* were reactivated from sclerotia before use because they contained few starch grains that can interfere with polarized light microscopy. Thin-spread plasmodia were prepared by the method of Kamiya and Kuroda (16) with slight modifications (11). The anterior regions of the thin-spread plasmodia were dissected with a scalpel to make fragments of discoid or ellipsoid shape, 100–200 μm in size. The fragments were overlaid with cover slips that were spaced with small pieces of cellophane film.

Light Microscopy

Living plasmodial fragments were examined with a differential interference microscope (Nikon Biophoto), and with a polarizing microscope (Nikon Apophoto) equipped with rectified strainfree optics and a Nikon Brace-Köhler type compensator (S_{546} = 1/20λ). The compensator was used by setting the angle usually at 5–6° on either side of extinction. For fluorescence microscopy, fragments were fixed on ice for 10 min in a improved fixing solution (9) consisting of 2% glutaraldehyde, 2% paraformaldehyde, 50 mM KCl, 25 mM EDTA, 0.5% Triton X-100, and 10 mM K-phosphate buffer (pH 7.0). Phases of the contraction–relaxation cycle of the fragments were ascertained with the polarizing microscope immediately before application of the fixative. The specimens were further fixed for 30 min at room

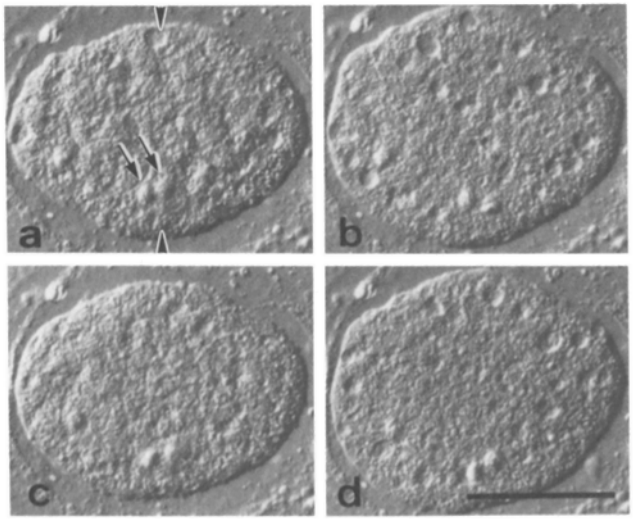

Figure 1. Sequential images showing a plasmodial fragment undergoing two successive contraction–relaxation cycles. (*a* and *c*) Maximum contraction; (*b* and *d*) maximum relaxation. The contractility can be monitored by the linear or area dimensions; the short axis (*a*, *arrowheads*) was shortened by 12% at maximum contraction; the area occupied by the fragment decreased by 9%. Cytoplasmic particles (*a*, *arrows*) showed reversible translocations only for a short distance coupled with the contraction cycles. Bar, 50 μm.

temperature in the fixing solution free of Triton X-100, washed in PBS, and stained for 20 min with rhodamine-phalloidin (Molecular Probes, Inc., Junction City, OR) diluted 20-fold with PBS. Observations were made with a fluorescence microscope (Nikon Optiphoto FEDA). Kodak Tri-X films were used and developed in Konidolsuper (Konishiroku, Inc., Tokyo) corresponding to ASA 3,200. For image analysis, micrographs of fine grain and of high contrast were obtained using Fuji Minicopy HR-II films (Fiji Photo Film Co., Ltd., Tokyo) that were processed in D19 developer. For fluometry of the fragments, 10 samples were fixed at the contraction and relaxation phases, respectively, and stained with 20-fold diluted rhodamine-phalloidin for 1 h. After overnight washing with PBS, fluorescent intensities were measured with a fluorescence microscope (Olympus IMT-2-21NR) equipped with a photoncounter (model C-1230 with a type 4645 phototube; Hamamatsu Phototonics K. K., Hamamatsu City, Japan). The measurement was completed within 1 s after opening the shutter of the light source to avoid photobleaching. Areas of the fragments were measured on the micrographs, and the thicknesses were obtained from the cross sections of the fragments embedded in epoxy resin. From these measurements, the fluorescent intensities per unit volume of the plasmodia were calculated.

Image Analysis

Image processing and analysis were done with a Nippon Avionics image processing system TVIP-2100 to determine the areas of the birefringent fibrils on the micrograph images recorded at 12-s intervals. The areas occupied by fragments were computed from their contours.

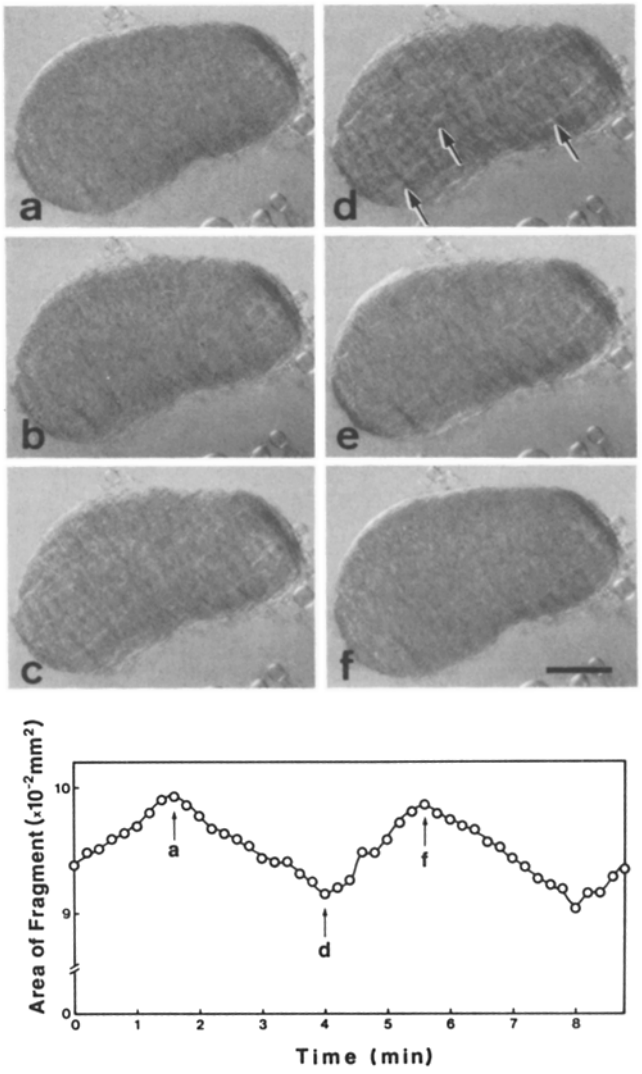

Figure 2. Sequential birefringent images of a plasmodial fragment at 48-s intervals that were selected from a series of photographs taken every 12 s. The fibrils develop during the contraction phase, finally attaining a highly organized structure (*d*) in which several fibrils converge at nodes indicated by arrows. The fibrils disappear almost completely at maximum relaxation (*a* and *f*). The graph shows changes of the area during two successive cycles of the same fragment. The a, d, and f in the graph indicate the areas of the fragment marked with the same letters in the micrographs. From this figure, it is easily recognized that the maximum contraction corresponds to the maximum amount of fibrils and the maximum relaxation to the minimum amount. Bar, 100 μm.

Results

Dynamic Behavior of the Plasmodial Fragment

The plasmodial fragments contracted–relaxed cyclicly over a period of 3-5 min for more than 30 min after amputation from the plasmodium. Fig. 1 shows two successive contraction cycles of a fragment, i.e., *a* and *c* represent the maximum phase of contraction, and *b* and *d* the maximum relaxation. The fragments bulged up during contraction and flattened during relaxation phase. Contraction and relaxation could be monitored as changes either in the linear or area dimensions; the short axis, indicated by the two arrowheads facing each other in Fig. 1 *a*, shortened by 12% at the maximum contraction, and the area was 9% smaller during contraction. The area was a better indicator of contractility than length, because it was more regular and because the shape changed gradually with time.

In most cases, the fragments showed no prominent endoplasmic streaming, suggesting that there was very little, if any, difference in the local internal pressure. Cytoplasmic particles showed reversible translocations only for short distances in accordance with the contraction cycles. They moved centripetally in the contraction phase and centrifu-

gally in the relaxation phase (Notice the particles marked with *arrows* in Fig. 1 *a*).

Cyclic Changes in the Fibrillar Organization of the Fragment by Polarizing Microscopy

We used polarizing microscopy to follow the rhythmic changes in the cytoplasmic actomyosin fibrils (Fig. 2). In the contraction phase, the fibrils appear and reinforce the birefringence as if some of the dispersed filamentous material are combined into substantial fibrils (Fig. 2 *d*). The fibrils usually intersect at many points (nodes) and form a three-dimensional framework like a birdcage, although they are detectable as two lattices intersecting each other at an angle of ~90° at any given setting of the polarizer and analyzer. In the relaxation phase, the birefringence of the fibrils gradually weakens as if they dissolve into the cytoplasm and disappear almost completely at the final stage (Fig. 2, *a* and *f*). Some of the fibrils show a tendency to remain near the nodes and the periphery. The birefringent changes are synchronized all over the fragment in most cases. The fibrils tend to appear at the same loci during a few cycles. Traces of a single fibril showed that the birefringence became gradually intense through a few strong–weak cycles and then diminished in the next few cycles. The area change of the same fragment has been examined during two successive cycles (see the graph of Fig. 2). The maximum contraction apparently coincides with the maximum amount of fibrils and the maximum relaxation with minimum amount. Such agreement was seen in almost all of the examined samples (~50 fragments).

Fibrillar Organization by Fluorescence Microscopy

The birefringent fibrils in the most contracted specimens were fixed by our procedures and were stained with rhodamine-phalloidin, which provides verification that they contain actin filaments (Fig. 3). The cytoplasmic actomyosin fibrils are located mainly in the dorsal layer (Fig. 3 *c*), composing a convex framework like a birdcage that entirely covers the dorsal layer of the fragment. There are fewer fibrils in the ventral layer (Fig. 3 *d*). Fibrils converge at nodes (*arrowheads* in Fig. 3, *c* and *d*). The middle layer of cytoplasmic sol between the dorsal and ventral cortical layers was stained evenly with rhodamine-phalloidin. In completely relaxed specimens, very few or no fibrils were stained (Fig. 4).

Fluorescent intensities of 10 specimens, stained with rhodamine-phalloidin, were examined for each phase. At the contraction phase, the fluorescent intensities ranged from 3.49 to 6.00 $\times$ 10^5 cps/mm^3. Mean value with a standard error was 4.59 $\pm$ 0.35 $\times$ 10^5 cps/mm^3. At the relaxation phase, they ranged from 2.32 to 6.14 $\times$ 10^5 cps/mm^3 (4.39 $\pm$ 0.34 $\times$ 10^5 cps/mm^3). These results indicate that the G-F transformation of actin is not the main underlying process of the fibrillogenesis.

Phase Relationship between the Generation Cycle of the Fibrils and the Contraction Cycle of the Fragment

We used image analysis to document quantitatively the phase relationship between the area of fragment and its content of fibrils (Figs. 5, 6, and 7). The peaks of fibril content appeared just after the maximum contraction, delayed only by ~3% of a normalized cycle. The minimum amount of fibrils cor-

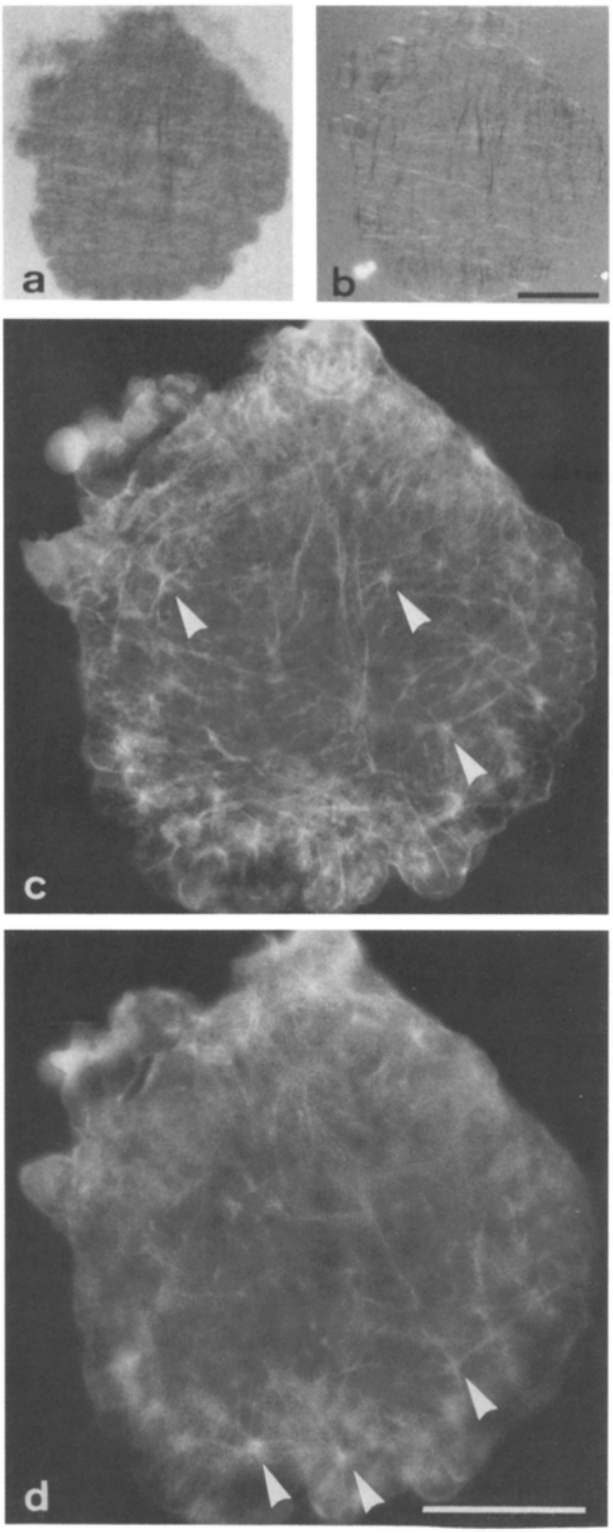

Figure 3. Fibrillar organization of a fragment at the maximum contraction phase. (*a* and *b*) Polarized light micrographs of the fragment immediately before application of the fixation solution (*a*) and after the fixing and staining procedures (*b*), respectively. These indicate that the fibrillar structure is favorably preserved throughout the procedures. (*c* and *d*) The fibrillar organizations in the dorsal and ventral cortical layers, respectively, that were revealed by rhodamine-phalloidin staining. More fibrils are seen in the dorsal layer than in the ventral layer. Several fibrils converge at one point, making the node structure (*arrowheads*). Bars, 100 μm.

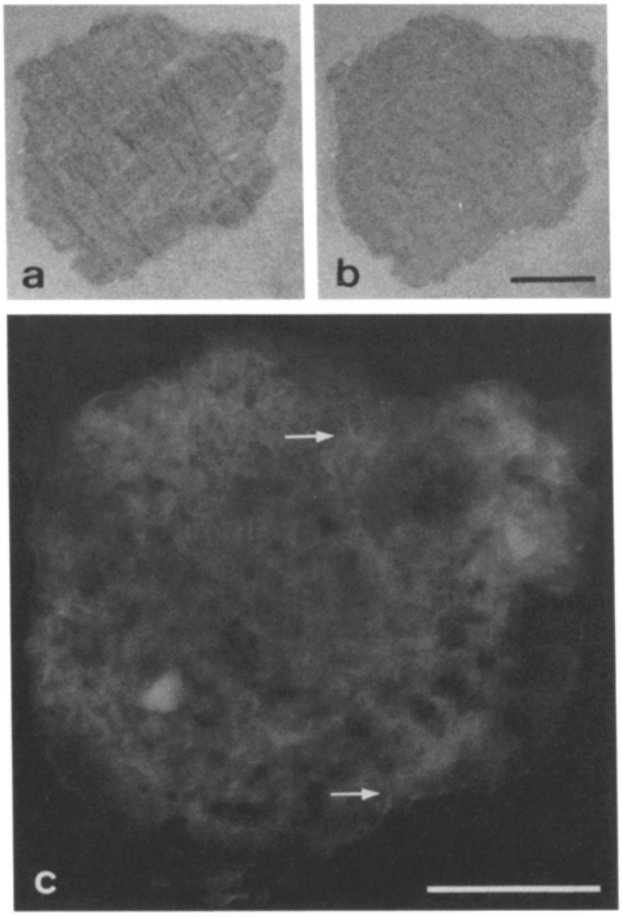

Figure 4. Cytoplasmic fibrils disappear almost completely at the maximum phase of relaxation. (*a* and *b*) In vivo birefringent patterns of the same fragment in a contraction phase and the subsequent relaxation phase, respectively. As soon as *b* was taken, the fragment was fixed and stained with rhodamine-phalloidin (*c*). Some weak fibrils can be observed near the node and the periphery (*arrows*). Bars, 100 μm.

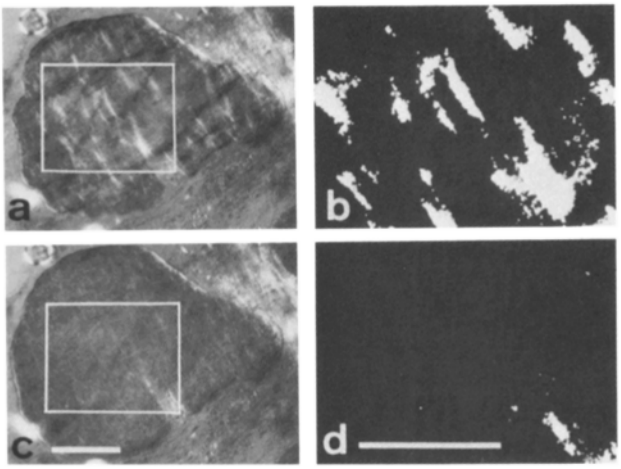

Figure 5. Images of birefringent fibrils before (*a* and *c*) and after (*b* and *d*) image processing. The positive birefringent fibrils in the given area (boxed areas in *a* and *c*) were reproduced as clusters of bright dots on a monitor, and ratios of the fibrillar areas to the boxed areas were computed. The fibrillar area occupied >10% of the boxed area at maximum contraction (*a* and *b*). Bars, 50 μm.

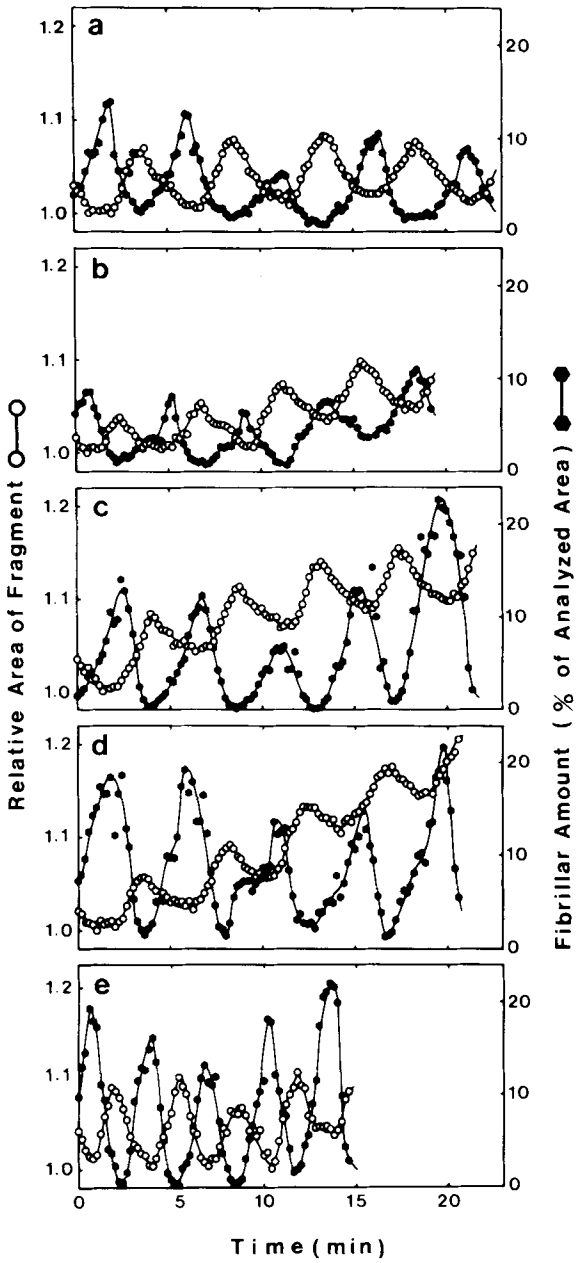

Figure 6. Phase relationship between fibrillar generation–degeneration and contraction–relaxation of the fragment. A total of 557 images, obtained from five cycles of five fragments (*a–e*) (25 cycles as a total), were analyzed. The smallest area of each fragment was regarded as 1.00; other data were normalized against this value. The maximum amount of fibrils corresponds to the maximum contraction (the minimum area) and that the minimum amount corresponds to the maximum relaxation (the maximum area). The time lags between the maximum amount of fibrils and the maximum contraction and between the minimum amount of fibrils and the maximum relaxation were very small as shown in Fig. 7.

responded within 1% of a cycle to the maximum relaxation (Figs. 6 and 7). These results strongly suggest that the cytoplasmic actomyosin fibrils develop with the progress of contraction, attaining a highly organized structure at maximum contraction, and that they disintegrate almost completely at maximum relaxation.

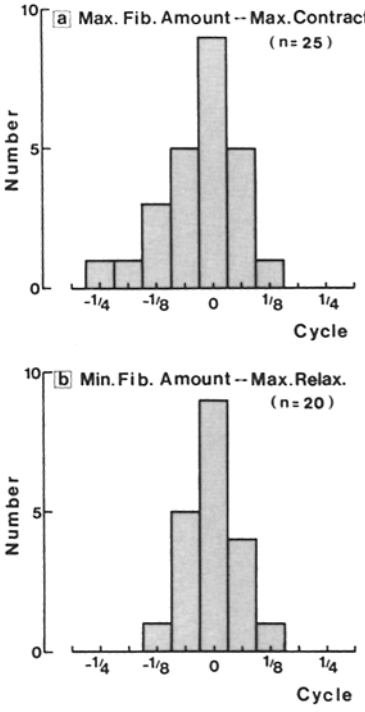

Figure 7. Histograms showing time lags between the maximum amount of fibrils and the maximum phase of contraction (*a*) and between the minimum amount and the maximum relaxation (*b*) represented in Fig. 6. They are grouped according to the ratio of time lag to the averaged period of one contraction cycle. Mean values with standard errors are -0.029 ± 0.020 ($n = 25$) in *a* and 0.004 ± 0.012 ($n = 20$) in *b*. Designation "plus" means that the peak of the fibrillar amount was ahead of that of the contraction or relaxation.

Discussion

The most developed fibrillar system occurs in the maximum contraction phase and not in the phase when the contraction rate is maximum. Kamiya and his co-workers (14, 24) found that the phase of maximum tension production corresponded to the shortest phase of the plasmodial strand and not to the phase of maximum shortening velocity, hereby offering evidence for the existence of a capacity similar to the tonic contraction in the molluscan catch muscle. Based on this interpretation, the developing process of cytoplasmic fibrils must be the substantial mechanism maintaining such a tonic contraction, and the most developed fibrils must generate a tonic tension. This explanation may offer suggestions for understanding the functions of fibrillar systems in other nonmuscle cells such as stress fibers (5, 22).

Using fluometry of plasmodial fragments stained with rhodamine-phalloidin, we have presented quantitative results suggesting that the cytoplasmic fibrils are formed depending on the changes in the aggregation pattern of F-actin. This indicates that some activities play a role in organizing F-actin filaments into three-dimensional network of the fibrils during the contraction phase. Short and weak fibrils tended to remain around the nodes through the relaxation phase. Similar structures in culture cells have been shown to act as converging points and to contain an actin-binding protein, α-actinin (20, 21). The roles and components of the node in the plasmodium need to be clarified for understanding the fibrillar dynamics.

As previously described (9, 11, 13, 25), the cytoplasmic fibrils in the anterior of a thin-spread plasmodium are generated when the endoplasm is streaming backward and degenerate in the reverse direction. In contrast, the fibrils in the posterior regions exhibit no rhythmic changes. Based on our findings that the fibrils form in the contraction phase of the plasmodium, we conclude that the shuttle streaming is caused by the periodic contraction of the anterior region (10, 32). The endoplasm may flow forward when the internal pressure of the anterior region becomes lower than that of the posterior, which remains nearly constant, and may flow backward when the pressure in the anterior becomes higher.

The plasmodial fragment system developed in this study is an advantageous model system for investigating nonmuscle cell motility, because it exhibits uniformity in contractility and synchrony in the morphodynamical behavior of the contractile apparatus. Furthermore, by using the microinjection technique, this system may offer good opportunities for more definite investigations with regard to the functions of the regulatory factors such as Ca^{2+} (1, 19, 28, 33, 34), nucleotides (29, 33), and actin-binding proteins (7, 26, 27).

The authors are grateful to Mr. T. Furuichi of Nippon Avionics Co., Ltd., Tokyo, for his expert technical assistance and advice during the course of the image analysis.

This work was supported in part by grants-in-aid for scientific research (projects 59380026 and 60114009) from the Japanese Ministry of Education, Science, and Culture.

Received for publication 11 September 1986, and in revised form 12 February 1987.

References

1. Achenbach, F., and K. E. Wohlfarth-Bottermann. 1986. Reactivation of cell-free models of endoplasmic drops from *Physarum polycephalum* after glycerol extraction at low ionic strength. *Eur. J. Cell Biol.* 40:135–138.
2. Alléra, A., and K. E. Wohlfarth-Bottermann. 1972. Weitreichende fibrilläre Protoplasmadifferenzierungen und ihre Bedeutung für die Protoplasmaströmung. IX. Aggregationszustände des Myosins und Bedingungen zur Entstehung von Myosinfilamenten in den Plasmodien von *Physarum polycephalum*. *Cytobiologie.* 6:261–286.
3. Alléra, A., R. Beck, and K. E. Wohlfarth-Bottermann. 1971. Weitreichende fibrilläre Protoplasmadifferenzierungen und ihre Bedeutung für die Protoplasmaströmung. VIII. Identifizierung der Plasmafilamente von *Physarum polycephalum* als F-Actin durch Anlagerung von heavy Meromyosin in situ. *Cytobiologie.* 4:437–449.
4. Beck, R., H. Hinssen, H. Komnick, W. Stockem, and K. E. Wohlfarth-Bottermann. 1970. Weitreichende fibrilläre Protoplasmadifferenzierungen und ihre Bedeutung für die Protoplasmaströmung. V. Kontraction, ATP-ase Activität und Feinstruktur isolierter Actomyosinfäden von *Physarum polycephalum*. *Cytobiologie.* 2:259–274.
5. Buckley, I. K., and K. R. Porter. 1967. Cytoplasmic fibrils in living cultured cells: a light and electron microscope study. *Protoplasma.* 64: 349–380.
6. Fleischer, M., and K. E. Wohlfarth-Bottermann. 1975. Correlation between tension force generation, fibrillogenesis and ultrastructure of cytoplasmic actomyosin during isometric and isotonic contractions of protoplasmic strands. *Cytobiologie.* 10:339–365.
7. Hasegawa, T., S. Takahashi, H. Hayashi, and S. Hatano. 1980. Fragmin: a calcium ion sensitive regulatory factor on the formation of actin filaments. *Biochemistry.* 19:2677–2683.
8. Isenberg, G., and K. E. Wohlfarth-Botterman. 1976. Transformation of cytoplasmic actin. Importance for the organization of the contractile gel reticulum and the contraction-relaxation cycle of cytoplasmic actomyosin. *Cell Tissue Res.* 173:495–528.
9. Ishigami, M. 1986. Dynamic aspects of the contractile system in *Physarum* plasmodium. I. Changes in spatial organization of the cytoplasmic fibrils according to the contraction-relaxation cycle. *Cell Motil. Cytoskeleton.* 6:439–447.
10. Ishigami, M., and S. Hatano. 1986. Dynamic aspects of the contractile system in *Physarum* plasmodium. II. Contractility of Triton cell models in accordance with the contraction and relaxation phases of the plasmodia. *Cell Motil. Cytoskeleton.* 6:448–457.
11. Ishigami, M., R. Nagai, and K. Kuroda. 1981. A polarized light and electron microscopic study of birefringent fibrils in *Physarum* plasmodia. *Protoplasma.* 109:91–102.
12. Kamiya, N. 1970. Contractile properties of the plasmodial strand. *Proc. Jpn. Acad.* 46:1026–1031.
13. Kamiya, N. 1973. Contractile characteristics of the myxomycete plasmodium. Proc. 4th Int. Biophys. Congr. (Moscow) Symp. III. Biophysics of Motility. 447–465.
14. Kamiya, N. 1979. Dynamic aspects of movement in the myxomycete plasmodium. *In* Cell Motility: Molecules and Organization. S. Hatano, H. Ishikawa, and H. Sato, editors. Tokyo University Press, Tokyo.

399–414.
15. Kamiya, N. 1981. Physical and chemical basis of cytoplasmic streaming. *Annu. Rev. Plant Physiol.* 32:205–236.
16. Kamiya, N., and K. Kuroda. 1965. Movement of the myxomycete plasmodium. I. A study of glycerinated models. *Proc. Jpn. Acad.* 41:837–841.
17. Kessler, D. 1972. On the location of myosin in the myxomycete *Physarum polycephalum* and its possible function in cytoplasmic streaming. *J. Mechanochem. Cell Motil.* 1:125–137.
18. Kessler, D. 1982. Plasmodial structure and motility. *In* Cell Biology of *Physarum* and *Didymium*. Vol. 1. H. C. Aldrich and J. W. Daniel, editors. Academic Press, Inc., New York. 145–208.
19. Kuroda, R., and H. Kuroda. 1981. Relation of cytoplasmic calcium to contractility in *Physarum polycephalum*. *J. Cell Sci.* 53:37–48.
20. Lazarides, E. 1976. Actin, α-actinin, and tropomyosin interaction in the structural organization of actin filaments in nonmuscle cells. *J. Cell Biol.* 68:202–219.
21. Lazarides, E., and K. Burridge. 1975. α-actinin: immunofluorescent localization of a muscle structural protein in nonmuscle cells. *Cell.* 6:289–298.
22. Lazarides, E., and K. Weber. 1974. Actin antibody: the specific visualization of actin filaments in non-muscle cells. *Proc. Natl. Acad. Sci. USA.* 71:2268–2272.
23. Nagai, R., and N. Kamiya. 1968. Movement of the myxomycete plasmodium. VI. Fibrillar structures in the glycerinated plasmodium. *Proc. Jpn. Acad.* 44:1044–1047.
24. Nagai, R., Y. Yoshimoto, and N. Kamiya. 1978. Cyclic production of tension force in the plasmodial strand of *Physarum* polycephalum and its relation to microfilament morphology. *J. Cell Sci.* 33:121–136.
25. Naib-Majani, W., F. Achenbach, K. Weber, K. E. Wohlfarth-Bottermann, and W. Stockem. 1984. Immunocytochemistry of the acellular slime mold *Physarum polycephalum*. IV. Differentiation and dynamics of the polygonal actomyosin system. *Differentiation*. 26:11–22.
26. Ogihara, S., and Y. Tonomura. 1982. A novel 36,000-dalton actin-binding protein purified from microfilaments in *Physarum* plasmodia which aggregates actin filaments and blocks actin-myosin interaction. *J. Cell Biol.* 93:604–614.
27. Ogihara, S., M. Ikebe, and Y. Tonomura. 1983. Requirement of phosphorylation of *Physarum* myosin heavy chain for thick filament formation, actin activation of Mg^{2+}-ATPase activity, and Ca^{2+}-inhibitory superprecipitation. *J. Biochem. (Tokyo)* 93:205–223.
28. Pies, N. J., and K. E. Wohlfarth-Bottermann. 1986. Reactivation of a cell-free model from *Physarum polycephalum*: studies on cryosections indicate an inhibitory effect of Ca^{2+} on cytoplasmic actomyosin contraction. *Eur. J. Cell Biol.* 40:139–149.
29. Ueda, T., K. Matsumoto, T. Akitaya, and Y. Kobatake. 1986. Spatial and temporal organization of intracellular adenine nucleotides and cyclic nucleotides in relation to rhythmic motility in *Physarum* plasmodium. *Exp. Cell Res.* 162:486–494.
30. Wohlfarth-Botterman, K. E. 1964. Differentiations of the ground cytoplasm and their significance for the generation of the motive force of ameboid movement. *In* Primitive Motile Systems in Cell Biology. R. D. Allen and N. Kamiya, editors. Academic Press, Inc. New York. 79–109.
31. Wohlfarth-Bottermann, K. E., and M. Fleischer. 1976. Cyclic aggregation patterns of cytoplasmic F-actin coordinated with oscillating tension force generation. *Cell Tissue Res.* 165:327–344.
32. Yoshimoto, Y., and N. Kamiya. 1978. Studies on contraction rhythm of the plasmodial strand. IV. Site of active oscillation in an advancing plasmodium. *Protoplasma.* 95:123–133.
33. Yoshimoto, Y., and N. Kamiya. 1984. ATP- and calcium-controlled contraction in a saponin model of *Physarum polycephalum*. *Cell Struct. Funct.* 9:135–141.
34. Yoshimoto, Y., F. Matsumura, and N. Kamiya. 1981. Simultaneous oscillations of Ca^{2+} efflux and tension generation in the permealized plasmodial strand of *Physarum*. *Cell Motil.* 1:433–443.